Some Ten-vertex *nido*-Metallaboranes: Oxidative Insertion of Iridium(I) and Rhodium(I) into the *arachno*-Nonaborate Anion, $[B_9H_{14}]^-$, and the Crystal and Molecular Structure of 6-Hydrido-6,6-bis(triphenylphosphine)-*nido*-6-iridadecaborane, $[(HIr^{III}B_9H_{13})(PPh_3)_2]$

By **Simon K. Boocock, Jonathan Bould, Norman N. Greenwood,* John D. Kennedy,** and **Walter S. McDonald,** Department of Inorganic and Structural Chemistry, University of Leeds, Leeds LS2 9JT

The *arachno*-anion $[B_9H_{14}]^-$ reacts with *trans*-$[Ir(CO)Cl(PPh_3)_2]$, *trans*-$[Ir(CO)Cl(PMe_3)_2]$, $[\{Ir(cod)Cl\}_2]$, and $[\{Rh(cod)Cl\}_2]$ (cod = cyclo-octa-1,5-diene) to give low yields of the *nido*-6-metalladecaboranes [6-H-6,6-$(PPh_3)_2$-*nido*-6-IrB_9H_{13}], [6-H-6,6-$(PMe_3)_2$-*nido*-6-IrB_9H_{13}], [6-$(\eta^2:\eta^2$-cod)-6-Cl-*nido*-6-IrB_9H_{13}], and [6-$(\eta^2:\eta^2$-cod)-6-Cl-*nido*-6-RhB_9H_{13}] respectively. These products have been characterized by single- and multiple-resonance n.m.r. spectroscopy and by single-crystal *X*-ray diffraction analysis on [6-H-6,6-$(PPh_3)_2$-*nido*-6-IrB_9H_{13}]. This last compound crystallizes in the orthorhombic space group $Pna2_1$, with a = 1 942.7(4), b = 1 196.7(2), c = 1 552.2(3) pm, Z = 4, and the structure (R = 0.024 for 2 333 observed reflections) of the metallaborane unit is that of a ten-vertex *nido*-cluster similar to that of $B_{10}H_{14}$, with the metal atom in the 6-position in the open face. The geometry about the iridium(III) atom is essentially octahedral, the metal being incorporated in the cluster *via* a direct Ir–B(2) bond and two Ir–H–B bridge bonds which differ in that one is *trans* to Ir–H(terminal) and the other *trans* to Ir–P.

THE metathetical reaction of simple iridium(I) compounds such as *trans*-$[Ir(CO)Cl(PPh_3)_2]$ with borane anions is often accompanied by an internal oxidative insertion of the metal atom into the borane cluster to form an iridium(III) or iridium(V) species with an expanded iridaborane cluster. For example, with the *nido*-$[B_5H_8]^-$ anion, the six-vertex *nido*-irida(III)hexaborane [2-(CO)-2,2-$(PPh_3)_2$-2-IrB_5H_8] is formed [equation (1)] [1] and with the *arachno*-$[B_3H_8]^-$ anion the four-vertex *arachno*-irida(V)tetraborane [1-(CO)-1-H-1,1-$(PPh_3)_2$-1-IrB_3H_7] is produced [equation (2)].[2] With

$$[Ir(CO)Cl(PPh_3)_2] + [B_5H_8]^- \longrightarrow [(IrB_5H_8)(CO)(PPh_3)_2] + Cl^- \quad (1)$$

$$[Ir(CO)Cl(PPh_3)_2] + [B_3H_8]^- \longrightarrow [(HIrB_3H_7)(CO)(PPh_3)_2] + Cl^- \quad (2)$$

closo-$[B_{10}H_{10}]^{2-}$ in methanol solution, the oxidative insertion may be accompanied by methanolic degradation and other condensation reactions to give species such as the ten-vertex *iso-nido*-irida(V)carbadecaborane $[(PPh_3)(PPh_2\overbrace{C_6H_4}^{}\overbrace{)(IrCB_8H_6}^{})(OMe)(OH)]$.[3] Sometimes, however, alternative degradative mechanisms compete, as for example in the formation (in low yields) of the fluxional five-vertex *arachno*-irida(III)pentaborane [1-(CO)-1,1-$(PMe_3)_2$-1-IrB_4H_9] from the reaction of *trans*-$[Ir(CO)Cl(PMe_3)_2]$ with either *nido*-$[B_9H_{12}]^-$ or *nido*-$[B_6H_9]^-$.[4] It is of obvious interest to extend a study of these reactions to include other borane anions, and here we report some results from the examination of the reaction of the *arachno*-nonaborate anion, $[B_9H_{14}]^-$, with some iridium(I) and rhodium(I) species.

RESULTS AND DISCUSSION

The reaction of *trans*-$[Ir(CO)Cl(PPh_3)_2]$ with the *arachno*-$[B_9H_{14}]^-$ anion for 24 h at room temperature in neutral dipolar solvents gives a small yield (<2%) of the yellow compound [6-H-6,6-$(PPh_3)_2$-*nido*-6-IrB_9H_{13}] (1), which may be separated and purified chromatographically. Although most of the $[B_9H_{14}]^-$ anion is used up during this period, and the bulk of the iridium starting complex recoverable, the yield of the iridadecaborane (1) is not substantially increased when an excess of $[B_9H_{14}]^-$ is used, when the counter ion is changed, or when a variety of other conditions are used. By contrast, the use of the trimethylphosphine complex *trans*-$[Ir(CO)Cl(PMe_3)_2]$ instead of the triphenylphosphine one results in an immediate reaction, but the yield of the corresponding bis(trimethylphosphine)iridadecaborane [6-H-6,6-$(PMe_3)_2$-*nido*-6-IrB_9H_{13}] (2), though improved, is still low (*ca.* 5%). In this case the major product of the reaction (50%) is the colourless neutral *arachno*-nonaborane ligand complex $[B_9H_{13}\cdot PMe_3]$. Other minor products from these reactions have been tentatively identified as being members of a series of nine-vertex *arachno*-, *nido*-, and *closo*-iridanonaborane species; these however appear from preliminary experiments to be more readily obtainable *via* other synthetic approaches, and we hope to describe their thorough characterisation in subsequent communications.

The low yields meant that insufficient quantities of the iridadecaboranes $[(HIrB_9H_{13})(PR_3)_2]$ (1) and (2) were available for elemental analysis. They did not yield satisfactory high-resolution mass spectra, and since their n.m.r. data were also insufficient for their characterisation, this was carried out by single crystal *X*-ray diffraction analysis on the bis(triphenylphosphine) compound (1), which yields orthorhombic crystals from dichloromethane–pentane. Details of the structure analysis and the atomic co-ordinates for (1) are given in the Experimental section. Selected interatomic distances are in Table 1 and angles between interatomic vectors in Table 2. All atoms were located, which confirms the formula as $[(HIrB_9H_{13})(PPh_3)_2]$, and an ORTEP drawing of the molecule is presented in Figure 1.

TABLE 1

Selected interatomic distances (pm) for $[(HIrB_9H_{13})(PPh_3)_2]$ (1) with estimated standard deviations in parentheses

(i) From the iridium atom			
Ir(6)–B(2)	226.9(8)	Ir(6)–H(6)	155(11)
Ir(6)–B(5)	228.9(9)	Ir(6)–H(5,6)	181(8)
Ir(6)–B(7)	228.1(11)	Ir(6)–H(6,7)	184(10)
Ir(6)–P(1)	230.3(2)	Ir(6)–P(2)	230.5(2)
(ii) Boron–boron			
B(1)–B(2)	180.4(13)	B(3)–B(2)	178.2(15)
B(1)–B(3)	178.8(14)		
B(1)–B(4)	180.6(14)	B(3)–B(4)	180.9(15)
B(1)–B(5)	173.4(13)	B(3)–B(7)	176.4(14)
B(1)–B(10)	172.8(14)	B(3)–B(8)	176.4(15)
B(2)–B(5)	183.0(11)	B(2)–B(7)	181.7(15)
B(4)–B(10)	176.8(14)	B(4)–B(8)	174.3(16)
B(4)–B(9)	170.4(15)		
B(5)–B(10)	199.7(16)	B(7)–B(8)	199.3(16)
B(9)–B(10)	177.9(17)	B(8)–B(9)	176.0(17)
(iii) Boron–hydrogen			
B(1)–H(1)	107(7)	B(3)–H(3)	105(7)
B(2)–H(2)	103(7)	B(4)–H(4)	120(7)
B(5)–H(5)	116(9)	B(7)–H(7)	124(7)
B(8)–H(8)	103(8)	B(10)–H(10)	105(8)
B(9)–H(9)	107(9)		
B(5)–H(5,6)	132(8)	B(7)–H(6,7)	154(8)
B(8)–H(8,9)	127(8)	B(10)–H(9,10)	117(9)
B(9)–H(8,9)	128(8)	B(9)–H(9,10)	113(9)
(iv) Phosphorus–carbon			
P(1)–C(1)	183.2(5)	P(2)–C(19)	182.1(5)
P(1)–C(7)	184.6(5)	P(2)–C(25)	183.1(5)
P(1)–C(13)	183.4(5)	P(2)–C(31)	183.6(5)

(v) Other

The phenyl rings were constrained to C–C 139.5 pm, C–H 108 pm, H–C–C 120°, and C–C–C 120°

TABLE 2

Selected angles (°) between interatomic vectors for $[(HIrB_9H_{13})(PPh_3)_2]$ (1), with estimated standard deviations in parentheses

(i) At the iridium atom			
P(1)–Ir(6)–P(2)	98.1(1)		
P(1)–Ir(6)–H(6)	81(3)	P(2)–Ir(6)–H(6)	91(3)
P(1)–Ir(6)–H(5,6)	177(2)	P(2)–Ir(6)–H(5,6)	83(3)
P(1)–Ir(6)–H(6,7)	100(3)	P(2)–Ir(6)–H(6,7)	86(2)
P(1)–Ir(6)–B(2)	101.5(2)	P(2)–Ir(6)–B(2)	159.6(3)
P(1)–Ir(6)–B(5)	143.1(2)	P(2)–Ir(6)–B(5)	115.9(2)
P(1)–Ir(6)–B(7)	89.0(3)	P(2)–Ir(6)–B(7)	128.2(3)
H(6)–Ir(6)–H(5,6)	97(4)	B(2)–Ir(6)–H(5,6)	78(3)
H(6)–Ir(6)–H(6,7)	177(3)	B(2)–Ir(6)–H(6,7)	85(2)
H(6)–Ir(6)–B(2)	97(3)	B(2)–Ir(6)–B(5)	47.3(3)
H(6)–Ir(6)–B(5)	85(3)	B(2)–Ir(6)–B(7)	47.1(4)
H(6)–Ir(6)–B(7)	140(3)		
H(5,6)–Ir(6)–H(6,7)	83(4)	H(6,7)–Ir(6)–B(5)	96(3)
H(5,6)–Ir(6)–B(5)	35(3)	H(6,7)–Ir(6)–B(7)	42(2)
H(5,6)–Ir(6)–B(7)	93(3)	B(5)–Ir(6)–B(7)	81.1(4)
(ii) Iridium–boron–boron			
Ir(6)–B(2)–B(1)	117.4(5)	Ir(6)–B(2)–B(3)	118.6(6)
Ir(6)–B(2)–B(5)	66.9(4)	Ir(6)–B(2)–B(7)	66.8(4)
Ir(6)–B(5)–B(1)	119.6(6)	Ir(6)–B(7)–B(3)	118.9(6)
Ir(6)–B(5)–B(2)	65.8(4)	Ir(6)–B(7)–B(2)	66.1(5)
Ir(6)–B(5)–B(10)	121.4(7)	Ir(6)–B(7)–B(8)	118.6(6)
(iii) Selected other angles			
B(5)–B(2)–B(7)	109.1(7)	B(8)–B(4)–B(10)	105.6(8)
Ir–P(1)–C(1)	113.1(2)	Ir–P(2)–C(19)	119.1(2)
Ir–P(1)–C(7)	116.1(2)	Ir–P(2)–C(25)	122.2(2)
Ir–P(1)–C(13)	117.2(2)	Ir–P(2)–C(31)	104.0(2)

The structure of the metallaborane unit is seen to be that of a *nido*-ten-vertex cluster as typified by *nido*-decaborane, $B_{10}H_{14}$, and contrasts to the '*iso-nido*' structure recently reported [3] for the only other example of an iridium-containing *nido*-ten-vertex species. The metal atom in (1) is in the 6-position and the compound is therefore analogous to the two previously reported *nido*-6-metalladecaboranes, *viz.* the orange-red anionic

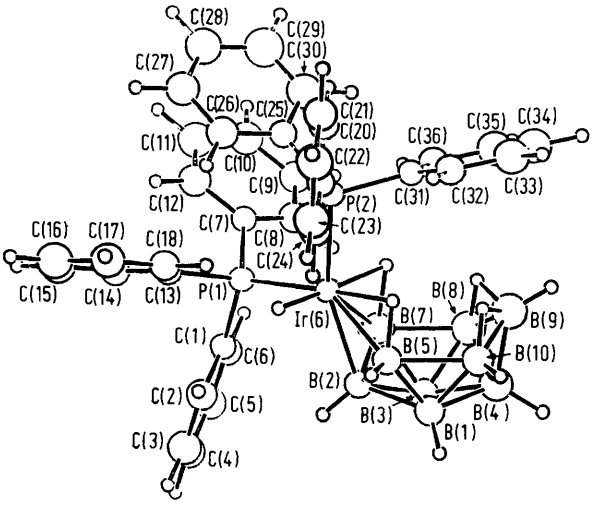

FIGURE 1 ORTEP drawing of $[6\text{-H-}6,6\text{-}(PPh_3)_2\text{-}nido\text{-}6\text{-}IrB_9H_{13}]$ (1). The cluster numbering is in the conventional manner

species $[(MnB_9H_{13})(CO)_3]^-$ and the violet neutral compound $[(CoB_9H_{13})(\eta^5\text{-}C_5H_5)]$.[5,6] In accord with this, the B–B and terminal B–H interatomic distances within the cluster are all within ranges typical for *nido*-ten-vertex species, and in particular are very similar to those [5,7] determined by single-crystal *X*-ray diffraction analysis for a number of neutral derivatives of the *nido*-6-manganadecaborane anion. As mentioned above, all hydrogen atoms were located, in particular the four cluster-bridging atoms. The electronic and atomic structure of the cluster is therefore very close to that of *nido*-decaborane, with the 6-$IrH(PPh_3)_2$ moiety taking the place of the decaborane 6-BH unit. Both will contribute three orbitals and two electrons to their respective cluster bondings, although there will of course be differences in orbital energies and also differences in angular disposition since the bonding at 6-$IrH(PPh_3)_2$ and 6-BH will involve $s + p^3 + d^2$ and $s + p^3$ combinations respectively.

The compound (1) is therefore reasonably formulated as an iridium(III) species, the co-ordination about the metal atom being essentially octahedral to the P(1), P(2), H(6), H(5,6), H(6,7), and B(2) atoms (Figure 1 and Table 2). The apparent distortion at the B(2) atom can be accounted for by the tangential nature of the bonding orbital overlap between the Ir(6) and B(2) atoms as represented in structure (I). The bonding Ir(6)–H(5,6)–B(5) and Ir(6)–H(6,7)–B(7) will be *via* 'open' three-centre Ir–H–B bonds and so the metal valencies are directed towards the H(5,6) and H(6,7) atoms. The

gross geometry about the manganese atom in the 6-manganadecaboranes [5,7] is very similar.

The detailed geometry about the metal atom in the iridium compound (1) merits some further comment. The two iridium–phosphorus distances Ir(6)–P(1) and Ir(6)–P(2) are essentially identical at 230.3(2) and 230.5(2) pm respectively, which indicates that the *trans*-lengthening effects [8] of the Ir(6)–B(2) bonding and the Ir(6)–H(5,6)–B(5) bridge bonding are similar. These distances

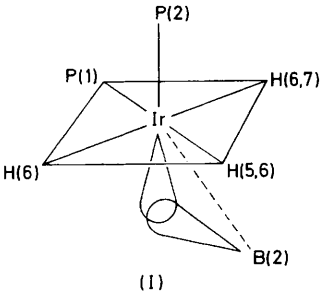

(I)

may be compared to those previously obtained [1] for the *quasi*-octahedral iridium(III) *nido*-metallahexaborane [2-(CO)-2,2-(PPh_3)$_2$-2-IrB_5H_8], in which the Ir–P distances for phosphorus atoms *trans* to an Ir–B two-electron two-centre bond and *trans* to an Ir–B two-electron three-centre bond are 240.0(1) and 234.9(1) pm respectively. *trans*-Influence should in principle be more marked in the distances from the metal atom to the bridging atoms H(5,6) and H(6,7), which are *trans* to the P(1) and H(6) atoms respectively. The well documented large *trans*-lengthening effect of a metal hydride bond may therefore be reflected in the longer distance Ir(6)–H(6,7) which exceeds that of Ir(6)–H(5,6) by *ca.* 3 pm. However, this particular variation is within experimental error, as are other apparent effects of this kind throughout the molecule.

These and other effects arising from the dissymmetry about the metal atom are more apparent in the n.m.r. behaviour of compounds (1) and (2) for which the ^{1}H, ^{11}B, and ^{31}P n.m.r. data are summarized in Tables 3 and 4. The ^{11}B resonances (Table 3) were initially assigned by analogy with the shieldings [9] in $B_{10}H_{14}$ (see Table 5 below) on the assumption that those boron nuclei nearest to the metal would show the greatest deviation in shielding from that of the parent borane.[5,7] The assignments are probably correct (see also the assignments below for the symmetrical derivatives 4 and 5) apart from some uncertainty among the B(5), B(7), B(1), and B(3) resonances, but since these are all close together their precise assignment is unimportant. The proton resonances were assigned to their directly bonded boron positions by selective ^{1}H-{^{11}B} spectroscopy,[10–12] and there is a general parallel between the ^{11}B and ^{1}H shielding of terminal B–H groups as previously observed in other polyhedral systems.[11–13]

The different *trans* influences about the iridium atom are manifest throughout the molecule, since the other-wise equivalent pairs of ^{11}B resonance positions differ by up to *ca.* 5 p.p.m., the largest deviations being at the B(5) and B(7) nuclei adjacent to the metal atom, as might be expected. This order of magnitude in the change of shielding probably represents differences in electronic environment about the boron nuclei involving 0.02 e$^-$ at the most,[14] and these variations in shielding

TABLE 3

Boron-11 and hydrogen-1 shielding data for the metallaborane clusters of [($HIrB_9H_{13}$)(PPh_3)$_2$] (1) and [($HIrB_9H_{13}$)(PMe_3)$_2$] (2) [a]

Tentative assignment [c] (atom position)	Compound (1) [b]		Compound (2) [b]	
	$\delta(^{11}B)$ [d]	$\delta(^1H)$ [e]	$\delta(^{11}B)$ [d]	$\delta(^1H)$ [e]
(9)	+13.2	+4.94	+10.5	+4.89
(1), (3)	+7.5	+4.33	+10.5	+4.56
	+9.0	+4.39	+9.2	+4.32
(5), (7) [g]	+10.5	+5.64	+8.1	+5.41
	+6.5	+3.14	+3.4	+3.27
(8), (10) [g]	−1.0	+3.05	−0.2	+3.04
	−4.8	+2.37	−2.2	+2.94
(2), (4)	−27.8	−0.99 [h]	−31.5	−0.40 [h]
	−27.5	+2.37 [i]	−31.5	+2.17 [i]
(8, 9)	—	−3.77	—	−3.69
(9, 10)	—	−4.58	—	−3.69
(6, 7) [j]	—	−6.64	—	−7.78
(5, 6)	—	−11.08	—	−10.60
(6)	Ir atom	−12.30	Ir atom	−13.03

[a] Terminal proton resonances assigned to corresponding ^{11}B resonances by selective ^{1}H-{^{11}B} experiments. [b] Dilute solution in $CDCl_3$ at +21 °C. [c] See text and Table 5, footnote *g*. [d] In p.p.m. ±0.5, to low field (high frequency) of BF_3·OEt_2. [e] In p.p.m. ±0.05, to low field (high frequency) of $SiMe_4$. [f] No differential selective sharpening apparent in ^{1}H-{^{11}B-(selective)} experiments. [g] Assigned by analogy with compounds (3) and (4) (see footnotes *g*, *n*, and *p* to Table 5). [h] Probably ^{1}H(4). [i] Probably ^{1}H(2). [j] Assigned *trans* to H(6-Ir) and thus to H(6,7) by selective ^{1}H-{^{11}B,^{1}H} spectroscopy (Figure 2).

are reflected in the (smaller) variations of shielding of the directly bonded terminal protons, as expected. The shieldings of the bridge protons H(8,9) and H(9,10) distant from the metal atom (Table 3) also differ somewhat, again as expected; this difference is much more marked for the triphenylphosphine compound (1) which presumably arises from the anisotropic shielding effects of the phenyl groups bonded to P(2).

The ^{1}H and ^{31}P resonances for the atoms about iridium in (1) and (2) (Table 4) were assigned by consideration of the magnitude of the various geminal *cis* and *trans* coupling constants $^2J(^{31}P–^{31}P)$, $^2J(^{31}P–^{11}B)$, $^2J(^{31}P–^1H)$, and $^2J(^1H–^1H)$, and by selective double and triple resonance experiments as summarized in the footnotes of Tables 3 and 4 and exemplified by Figure 2. The differences in shielding between the bridging protons ^{1}H(5,6) and ^{1}H(6,7) associated with the metal centre are large: that *trans* to the P(2)-phosphine ligand is within ranges normal for an M–H–B bridging position (*e.g.* Table 5, below), but that *trans* to the terminal Ir-hydrogen atom is some 3—4 p.p.m. less shielded; *i.e.* much more terminal in character, reflecting the large *trans*-influence of the metal hydride H(6).

The straightforward stoicheiometry of the equation

that can be written down for the formation of (1) and (2) [equation (3)] perhaps implies that the mechanism of formation of these compounds is straightforward, arising from an initial attack and addition of the metal centre at

$$[Ir(CO)Cl(PR_3)_2] + [B_9H_{14}]^- \longrightarrow [(HIrB_9H_{13})(PR_3)_2] + CO + Cl^- \quad (3)$$

the 6,7,8-positions of the *arachno*-nonaborane skeleton (II, equation 4) to give the observed product ten-vertex

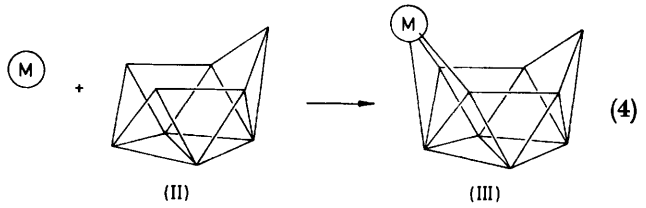

(II) (III) (4)

TABLE 4

Selected ^{31}P and ^1H n.m.r. data for $[(HIrB_9H_{13})(PPh_3)_2]$ (1) and $[(HIrB_9H_{13})(PMe_3)_2]$ (2) [a]

Parameter	Compound (1)	Compound (2)
$\delta[^{31}P(1)]$/p.p.m. [b]	+19.2 ± 0.5 [c]	−29.6 ± 0.5 [d]
$\delta[^{31}P(2)]$/p.p.m. [b]	+14.6 ± 0.5 [c]	−33.3 ± 0.5 [d]
$\delta(^1H)(PMe_3)$/p.p.m. [e,f]	—	(*i*) +1.83, (*ii*) +1.66
$\delta[^1H(6)]$/p.p.m. [e,f]	−12.30	−13.03
$\delta[^1H(5,6)]$/p.p.m. [e,f]	−11.08	−10.60
$\delta[^1H(6,7)]$/p.p.m. [e,f]	−6.64	−7.78
$^2J(^{31}P-^{31}P)(cis)$/Hz	21 ± 2 [c]	27 ± 2 [d]
$^2J(^{31}P-^1H)(PMe_3)$/Hz	—	(*i*) 10.7 ± 0.5, (*ii*) 9.7 ± 0.5
$^2J[^{31}P(1)-^1H(5,6)]$ (*trans*)/Hz [g]	66 ± 3	59 ± 3
$^2J[^{31}P(1)-^1H(6)](cis)$/Hz	18 ± 2	17 ± 2
$^2J[^{31}P(2)-^1H(6)](cis)$/Hz	19 ± 2	25 ± 2
$^2J[^{31}P(2)-^1H(5,6)](cis)$/Hz	<*ca.* 6	8 ± 4
$^2J[^1H(6)-^1H(6,7)](trans)$/Hz [h]	6.5 ± 0.5	8.8 ± 0.2

[a] Dilute solutions in $CDCl_3$ at +21 °C unless otherwise indicated. [b] $\delta(^{31}P)$ to low field (high frequency) of 85% H_3PO_4. [c] δ and J measured at −47 °C; at +21 °C, $w_{\frac{1}{2}}[P(1)]$ *ca.* 6 Hz, $w_{\frac{1}{2}}[P(2)]$ *ca.* 16 Hz; broader peak P(2) assigned *trans* to B(2), sharper peak P(1) *trans* to H(5,6). [d] At −40 °C; $w_{\frac{1}{2}}[P(1)]$ 7.5 Hz, $w_{\frac{1}{2}}[P(2)]$ *ca.* 30 Hz; peaks assigned as in footnote *c*. [e] $\delta(^1H)$ ± 0.05 p.p.m., to low field (high frequency) of $SiMe_4$. [f] No *cisoid* coupling $^4J(^1H-Ir-P-C-^1H)$ apparent. [g] Coupling to P(1) assigned by selective $^1H-\{^{31}P\}$ experiments; large magnitude confirms *trans* disposition. [h] See footnote *j* of Table 3.

geometry (III, equation 4). An addition of this type would initially yield an *arachno*-ten-vertex intermediate [equation (5)] which would then presumably lead to (1) and (2) *via* a hydride shift resulting in the formation of

$$[Ir(CO)Cl(PR_3)_2] + [B_9H_{14}]^- \longrightarrow [(HIrB_9H_{13})(CO)(PR_3)_2] + Cl^- \quad (5)$$

$$[(HIrB_9H_{13})(CO)(PR_3)_2] \longrightarrow [(HIrB_9H_{13})(PR_3)_2] + CO \quad (6)$$

the Ir–H–B bridges and a consequent internal substitution at Ir with elimination of the CO ligand [equation (6)]; the directional requirements of this elimination may perhaps account for the asymmetric distribution of the $(PR_3)_2H$ grouping about the metal atom.

However, this type of rationale is probably oversimplified, since yields are low, and reaction of the $[B_9H_{14}]^-$ anion with the dimeric iridium(I) and rhodium(I) species $[\{Ir(cod)Cl\}_2]$ and $[\{Rh(cod)Cl\}_2]$ respectively (cod = cyclo-octa-1,5-diene) does not give the straightforward hydridometallaboranes $[(HIrB_9H_{13})(cod)]$ and $[(HRhB_9H_{13})(cod)]$ that would otherwise be expected on the basis of equation (7). Instead, the only *nido*-

$$\tfrac{1}{2}[\{M(cod)Cl\}_2] + [B_9H_{14}]^- \longrightarrow [(HMB_9H_{13})(cod)] + Cl^- \quad (7)$$

metalladecaborane products that we have been able to obtain from this reaction are the orange-red halogenometalladecaboranes $[6\text{-}(\eta^2{:}\eta^2\text{-cod})\text{-}6\text{-}Cl\text{-}nido\text{-}6\text{-}IrB_9H_{13}]$ (3) and $[6\text{-}(\eta^2{:}\eta^2\text{-cod})\text{-}6\text{-}Cl\text{-}nido\text{-}6\text{-}RhB_9H_{13}]$ (4) respectively, and again these are formed in very low yields of <5%.

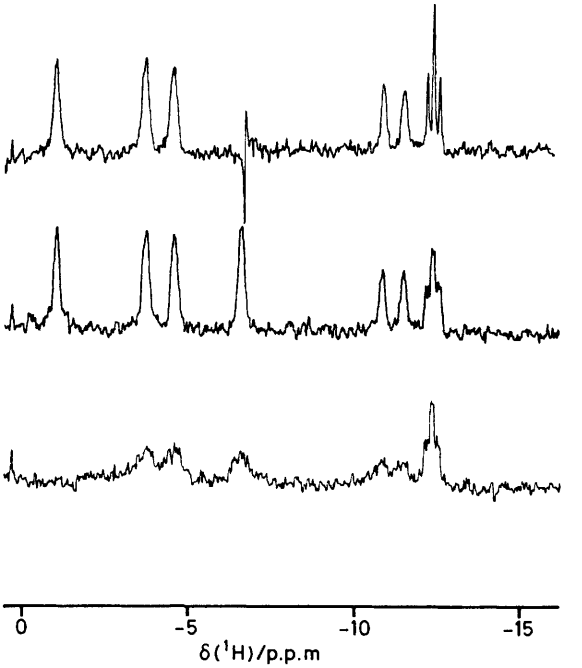

FIGURE 2 High-field (low-frequency) region of 100-MHz single- and multiple-resonance ^1H n.m.r. spectra of $[(HIrB_9H_{13})(PPh_3)_2]$ (1) in $CDCl_3$ solution at +21 °C. Lowest trace, straightforward single-resonance spectrum; centre trace, double resonance spectrum with simultaneous $\{^{11}B(broad\ band\ noise)\}$ decoupling; top trace, triple resonance spectrum with both simultaneous $\{^{11}B(broad\ band\ noise)\}$ decoupling and also $\{^1H(selective)\}$ irradiation at $\nu(^1H)$ corresponding to $\delta[^1H(6,7)] = 6.64$ p.p.m.; this shows and confirms the presence of $^2J[^1H(6)-Ir-^1H(6,7)] = 6.5 \pm 0.5$ Hz, and thus establishes the mutual disposition of H(6) and H(6,7) as *trans*

These compounds (3) and (4) were identified principally by their ^{11}B and ^1H n.m.r. spectra (Figure 3 and Table 4), which, by comparison with those for (2) and (3) (Table 3) and also for the previously reported [5,6] *nido*-6-metalladecaborane species $[(MnB_9H_{13})(CO)_3]^-$ and $[(CoB_9H_{13})(\eta^5\text{-}C_5H_5)]$, showed that they are also *nido*-6-metalladecaboranes and that they have a symmetrical disposition of ligands about the metal atom (Figures 3 and 4). The diamagnetic nature of the compounds together with the absence of an Ir-terminal hydride or Rh-terminal hydride resonance in the ^1H n.m.r. spectra of

TABLE 5

Boron-11 and proton n.m.r. data for [(ClIrB$_9$H$_{13}$)(cod)] (3) and [(ClRhB$_9$H$_{13}$)(cod)] (4) together with comparison data for related compounds

Tentative assignment	compound (3) [a]		compound (4) [a]		[(MnB$_9$H$_{13}$)(CO)$_3$]$^-$ [b]		[(CoB$_9$H$_{13}$)(η-C$_5$H$_5$)] [c]		B$_{10}$H$_{14}$ [d]	
	δ(^{11}B) [e,f,g]	δ(^{1}H) [h,i,j]	δ(^{11}B) [e,f,g]	δ(^{1}H) [h,i]	δ(^{11}B) [e,k]	δ(^{1}H) [h,l]	δ(^{11}B) [e,m]	δ(^{1}H) [h,j]	δ(^{11}B) [e]	δ(^{1}H) [h,j]
(5), (7)	+15.9 [n]	+5.84 [n]	+16.1 [n]	+4.69 [n]	+9.2	+3.8	+17.6	*o*	+0.7	+3.13
(1), (3)	+10.7	+4.71	+12.6	+3.91	+10.8	+3.8	+21.1	*o*	+11.3	+3.69
(9)	+10.0	+3.72	+9.0	+3.49	+0.1	+3.3	+7.2	*o*	+9.7	+3.85
(8), (10)	−2.5 [p]	+2.97 [p]	−1.5	+2.94	−1.8	+2.7	−2.0	*o*	+0.7	+3.13
(2)	−27.7	+2.51	−20.7	+0.49	−27.6	+0.5	−16.0	*o*	−35.8	+0.65
(4)	−30.6	−0.13	−26.4	−1.59	−34.3	−0.8	−26.3	*o*	−35.8	+0.65
(8, 9), (9, 10)	—	−3.08 [p]	—	−2.65 [p]	—	−3.0	—	−3.25	—	−2.14
(5, 6), (6, 7)	—	−10.05 [n]	—	−9.23 [n,q]	—	−11.4	—	−12.78	—	

[a] Dilute solution in $CDCl_3$ at +21 °C. [b] From ref. 5; solution of $[NMe_4][(CO)_3(MnB_9H_{13})]$ containing CD_3CN or CD_2Cl_2. [c] From ref. 6. [d] From refs. 9 and 11; solution in $CDCl_3$. [e] δ(^{11}B) in p.p.m. to high frequency (low field) of BF_3·OEt_2. [f] δ(^{11}B) ± 0.5 p.p.m. [g] Assignments based on comparison with $B_{10}H_{14}$ and the assumption that δ(^{11}B) of those nuclei nearest the metal atom will be shifted most; see also footnotes *n* and *p*. [h] δ(^{1}H) in p.p.m. to high frequency (low field) of $SiMe_4$. [i] δ(^{1}H) ± 0.05 p.p.m.; terminal ^{1}H resonances related to ^{11}B resonances of directly bonded B atoms by selective ^{1}H-{^{11}B} experiments. [j] Also δ(^{1}H) (cod) centred at +4.11, +3.09, +1.60, +1.43, +1.25, and +1.02 p.p.m. [k] Assigned in ref. 5, using the criteria of footnote *g* above. [l] Values from ^{1}H-{^{11}B} spectra in ref. 5; tentatively assigned by us based on the known parallels between δ(^{11}B) and δ(^{1}H) [*e.g.* refs. 11—13] and comparison with data for compounds (3) and (4). [m] Values from ref. 6, tentatively assigned by us. [n] Selective sharpening of the signals of ^{1}H(5), (7) and ^{1}H(5,6), (6,7) in a selective ^{1}H-{^{11}B(5), (7)} experiment confirms assignments. [o] Not reported. [p] Selective sharpening of the signals of ^{1}H(8,10) and ^{1}H(8,9),(9,10) in a selective ^{1}H{^{11}B(8), (10)} experiment confirms assignments. [q] $^1J(^{103}Rh-^1H) = 27 \pm 2$ Hz.

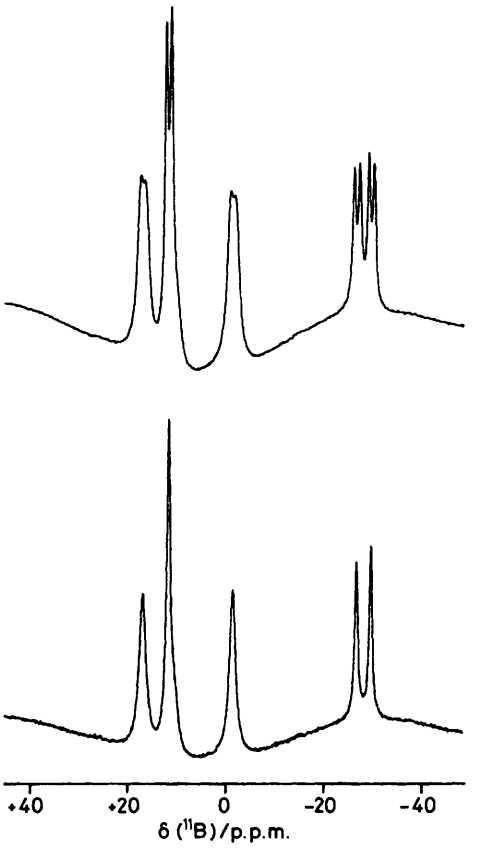

FIGURE 3 128-MHz ^{11}B n.m.r. spectra of [6-(η^2:η^2-cod)-6-Cl-*nido*-6-IrB$_9$H$_{13}$] (3) in $CDCl_3$ solution at +25 °C. Upper trace, normal ^{11}B spectrum; lower trace, with simultaneous {^{1}H (broad band noise)} decoupling. The upper trace was drawn with twice the recorder *Y*-gain compared to the lower trace. The resonance agglomerate of intensity 3 at δ(^{11}B) *ca.* +10 p.p.m. was resolved into two resonances of intensity 2 : 1 (Table 5) by line-narrowing and also (refs. 11—13) by selective ^{1}H-{^{11}B} spectroscopy. The overall 2 : 2 : 1 : 2 : 1 : 1 intensity ratio and lack of further multiplicity indicate symmetrically disposed ligands about the metal atom (see Figure 4)

compounds (3) and (4) indicated that there was probably a chlorine or other univalent atom associated with the metal atom in each case. Because of the small scale of the reactions and the small yields full elemental analyses were not possible, but sufficient material was available for the iridium compound (3) to confirm that the additional metal-atom substituent was indeed chlorine.

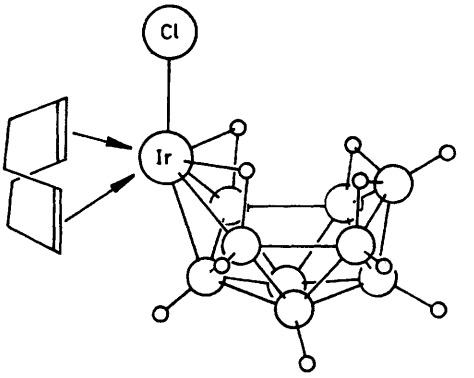

FIGURE 4 Representation of the proposed molecular structure of [(ClIrB$_9$H$_{13}$)(cod)] (3)

The n.m.r. data for comparable compounds are also given in Table 5. In the ^{1}H spectra the M–H–B resonance positions are remarkably similar for the four different metals Ir, Rh, Co, and Mn involved in the clusters, and the H(8,7) and H(9,10) B–H–B resonances are also very similar [with the exception of one of those for compound (1) which is discussed above]. Once more, as mentioned above for (1) and (2), in general the proton shieldings of terminal H atoms approximately parallel the nuclear shieldings of the B atoms to which they are attached. The ^{11}B resonances are generally somewhat less shielded than those of $B_{10}H_{14}$. Lower field shielding of boron nuclei appears to be a general phenomenon for metallaboranes,[15] and may be related to lower excitation energies associated with the metal centre which would

lead to larger 'paramagnetic' contributions to the shielding. However, these shielding processes are not well understood, particularly for polyhedral species, and in the present work this is illustrated by the comparative shielding differences throughout the cluster for the various species in Tables 3 and 5. There is no clear pattern to the changes as the metal centre is varied, and in particular the cobalt compound $[(CoB_9H_{13})(\eta^5\text{-}C_5H_5)]$ exhibits large deviations.

EXPERIMENTAL

General.—Metal starting complexes were prepared by standard methods and the $[B_9H_{14}]^-$ anion was prepared as previously described.[12] Reactions were carried out, and solids and solutions generally kept, under an atmosphere of dry nitrogen, although manipulations and separatory procedures were carried out in air. Preparative and analytical thin-layer chromatography (t.l.c.) were carried out using silica gel G (Fluka type GF 254) as the stationary phase, using general procedures described in more detail in previous reports from these laboratories.[12,16,17] Infrared spectra were recorded on a Perkin-Elmer 457 instrument and values quoted are ± 10 cm^{-1}.

N.M.R. Spectroscopy.—100-MHz ^{1}H, 40-MHz ^{31}P, and 32-MHz ^{11}B spectroscopy were carried out using a JEOL FX100 instrument. Selective ^{1}H-{^{11}B} double resonance experiments were carried out as previously described.[10-12] Irradiation at $\nu(^{11}B)$ for ^{1}H-{^{11}B,^{1}H} triple-resonance experiments was provided by a Fluke 6160A/DX frequency synthesiser together with a frequency doubler and square-wave noise generator built in these laboratories. The spectrometer 32-MHz amplifier was used and maximum power levels obtained for {^{11}B(broad band noise)} decoupling experiments were of the order of $\gamma B_2/2\pi = 3\,000$ Hz; power levels found useful for ^{1}H-{^{11}B(selective)} experiments[10-12] on the compounds described in this work were of the order of $\gamma B_2/2\pi = 500$ Hz, these values being estimated on the basis of off-resonance residual splittings as described in ref. 18. Continuous-wave irradiation at $\nu(^1H)$ for selective {^{1}H} irradiation in the ^{1}H-{^{11}B,^{1}H} mode was provided by the standard spectrometer units and fed into the pulser coils in the probe *via* a balanced mixer. 128-MHz ^{11}B spectra were recorded using a Bruker WH400 instrument at the University of Sheffield.

Synthesis of [6-H-6,6-$(PPh_3)_2$-*nido*-6-IrB_9H_{13}] (1).—*trans*-$[Ir(CO)Cl(PPh_3)_2]$ (0.385 g, 0.5 mmol) and $[NBu^t_4][B_9H_{14}]$ (0.21 g, 0.6 mmol) in CH_2Cl_2 (50 cm^3) were stirred at room temperature for 24 h, then filtered, yielding unreacted $[Ir(CO)Cl(PPh_3)_2]$ as a yellow solid (0.275 g, 0.40 mmol, 94% recovered). The orange solution was reduced in volume (rotary evaporator) and subjected to preparative t.l.c. separation using dichloromethane–light petroleum (b.p. 40—60 °C) (1 : 1) as the liquid phase. A number of components were separable within the range R_f 0.55—0.75 which have been tentatively identified as iridanonaborane species. A component at R_f 0.50 was identified as described in the Results and Discussion section above as [6-H-6,6-$(PPh_3)_2$-*nido*-6-IrB_9H_{13}] (1), bright orange-yellow crystals (4 mg, 0.005 mmol, *ca.* 1.0% yield), $\nu_{max.}$ 2 100, ν(Ir–H); 2 540, ν(B–H); and 2 480 cm^{-1}, ν(M–H–B).

Synthesis of [6-H-6,6-$(PMe_3)_2$-*nido*-6-IrB_9H_{13}] (2).—*trans*-$[Ir(CO)Cl(PMe_3)_2]$ (0.24 g, 0.60 mmol) was added to a stirred solution of $[NBu^t_4][B_9H_{14}]$ (0.21 g; 0.6 mmol) in CH_2Cl_2 (50 cm^3) at room temperature. The colour changed immediately from yellow to orange. The solution was reduced in volume, and preparative t.l.c. using dichloromethane–light petroleum (b.p. 40—60 °C) (1 : 1) as the liquid phase yielded *arachno*-$[B_9H_{13}\cdot PMe_3]$ as a white solid (0.06 g, 0.3 mmol, 50%; R_f 0.8) and [6-H-6,6-$(PMe_3)_2$-*nido*-6-IrB_9H_{13}] (2) as a yellow microcrystalline solid (13 mg, 0.03 mmol, 5%; R_f 0.5). A third component (13 mg, 0.03 mmol; R_f 0.7) has been tentatively identified as the iridium species [4-(CO)-4-H-4,4-$(PMe_3)_2$-*arachno*-4-IrB_8H_{12}], for which we hope to report a more complete characterisation in the near future.

Synthesis of [6-(η^2:η^2-cod)-6-Cl-*nido*-6-MB_9H_{13}] (3; M = Ir) *and* (4; M = Rh).—$[\{Ir(cod)Cl\}_2]$ (0.17 g, 0.5 mmol) was added to a stirred solution of $[NBu^t_4][B_9H_{14}]$ (0.18 g, 0.5 mmol) in CH_2Cl_2 (10 cm^3). Effervescence occurred for *ca.* 2 min, during which time the colour of the solution changed from the orange of $[\{Ir(cod)Cl\}_2]$ to dark red-black. The solution was reduced in volume and preparative t.l.c. using CH_2Cl_2 as the liquid phase yielded [6-(η^2:η^2-cod)-6-Cl-*nido*-6-IrB_9H_{13}] (3) as a red-orange solid (10 mg, 0.024 mmol, 5%; R_f 0.3) (Found: Cl, 8 ± 1% (0.4 mg sample). $C_8H_{25}B_9ClIr$ requires Cl, 7.9%). An identical procedure using $[\{Rh(cod)Cl\}_2]$ (0.06 g, 0.25 mmol) instead of the Ir analogue yielded [6-(η^2:η^2-cod)-6-Cl-*nido*-6-RhB_9H_{13})] (4) also as a red-orange solid (3.4 mg, 0.014 mmol, 5%; R_f 0.3). Both compounds were further characterised as described in the Results and Discussion section.

X-*Ray Diffraction Analysis.*—Recrystallisation of [6-H-6,6-$(PPh_3)_2$-*nido*-6-IrB_9H_{13}] (1) from dichloromethane–pentane yielded yellow-orange crystals suitable for single-crystal *X*-ray diffraction analysis.

Crystal data. $C_{36}H_{44}B_9IrP_2$, M = 828.2, Orthorhombic, a = 1 942.7(4), b = 1 196.7(2), c = 1 552.2(3) pm, U = 3.6086(10) nm^3, Z = 4, D_c = 1.524 Mg m^{-3}, $F(000)$ = 1 648, space group $Pna2_1$, Mo-K_α radiation, λ = 71.069 pm, μ(Mo-K_α) = 3.798 mm^{-1}.

Structure determination. Measurements were made on a Syntex $P2_1$ diffractometer. Cell dimensions were determined by least-squares treatment of the setting angles of 15 reflections with $35 < 2\theta < 40°$. Intensities of all independent reflections to $2\theta = 45°$ were measured in the ω—2θ scan mode with scan speeds varying between 1 and 29° min^{-1} according to a pre-scan intensity and running from 1° below $K_{\alpha1}$ to 1° above $K_{\alpha2}$. The structure analysis used the 2 333 reflections having $I > 3\sigma(I)$; 141 below this threshold were rejected as 'unobserved.' Correction for Lorentz, polarisation, and transmission factors, solution using Patterson and difference syntheses, and full-matrix least-squares refinement with anisotropic temperature factors for Ir and P and isotropic parameters for C and B gave R = 0.032. Since the space group is polar the structure of opposite polarity was also refined, giving R = 0.037, and was therefore rejected. A difference map revealed most of the hydrogen atoms, but one of those bonded to Ir was not clearly resolved. At this stage the computations were transferred to the SHELX programs, allowing the inclusion of the phenyl groups, including their hydrogens, as idealized rigid groups with C–C = 139.5 pm, C–H = 108 pm. This reduced R to 0.028 and a difference map now clearly revealed the 14 hydrogens of the iridaborane cluster. These were included in the refinement and their co-ordinates allowed to refine, although the isotropic temperature factors of all hydrogens were fixed at $U_{iso.}$ = 500 pm^2. Final

TABLE 6

Atomic parameters with estimated standard deviations in parentheses

Atom *	*x/a*	*y/b*	*z/c*
B(1)	0.028 9(5)	−0.173 5(8)	−0.045 8(7)
B(2)	−0.057 5(4)	−0.172 5(6)	−0.003 2(8)
B(3)	−0.040 2(5)	−0.235 3(8)	−0.105 1(6)
B(4)	0.032 3(6)	−0.176 1(9)	−0.162 1(7)
B(5)	0.000 8(4)	−0.052 7(6)	0.004 9(9)
Ir(6)	−0.113 44(1)	−0.006 12(2)	0
B(7)	−0.114 8(5)	−0.152 2(9)	−0.094 4(8)
B(8)	−0.051 6(6)	−0.147 8(9)	−0.195 5(8)
B(9)	0.014 0(7)	−0.046 7(10)	−0.201 8(8)
B(10)	0.058 2(6)	−0.058 0(9)	−0.101 7(7)
P(1)	−0.220 8(1)	−0.059 3(1)	0.047 5(2)
P(2)	−0.137 4(1)	0.179 2(2)	−0.027 0(2)
H(1)	0.074(4)	−0.213(6)	−0.020(5)
H(2)	−0.066(4)	−0.221(6)	0.051(5)
H(3)	−0.056(4)	−0.317(6)	−0.121(5)
H(4)	0.074(4)	−0.224(6)	−0.205(5)
H(5)	0.031(5)	−0.023(6)	0.065(6)
H(6)	−0.105(4)	0.018(6)	0.097(7)
H(7)	−0.162(4)	−0.215(6)	−0.118(5)
H(8)	−0.077(4)	−0.187(6)	−0.245(5)
H(9)	0.033(5)	−0.004(6)	−0.258(7)
H(10)	0.110(4)	−0.038(7)	−0.090(6)
H(56)	−0.028(4)	0.035(7)	−0.032(5)
H(67)	−0.124(4)	−0.028(7)	−0.117(6)
H(89)	−0.052(4)	−0.044(7)	−0.209(5)
H(910)	0.025(5)	0.005(6)	−0.142(7)

* The phenyl groups were refined as rigid groups with C–C = 139.5 pm, C–H = 108 pm, C–C–C and C–C–H = 120°. The parameters of these atoms are in SUP 23241.

convergence was at $R = 0.024$, $R' = 0.032$. The atomic co-ordinates and their standard deviations are given in Table 6. Observed and calculated structure factors and the vibration parameters are in Supplementary Publication No. SUP 23241 (21 pp.).*

* For details see Notices to Authors No. 7, *J. Chem. Soc., Dalton Trans.*, 1981, Index issue.

We thank Dr. D. Reed for some preliminary work on this system, the S.R.C. (S.E.R.C.) for support and for a Maintenance Grant (to J. B.), the University of Leeds for a Studentship (to S. K. B.), and Mr. A. Hedley for microanalysis.

[1/1650 *Received*, 23*rd October*, 1981]

REFERENCES

1 N. N. Greenwood, J. D. Kennedy, W. S. McDonald, D. Reed, and J. Staves, *J. Chem. Soc., Dalton Trans.*, 1979, 117.
2 N. N. Greenwood, J. D. Kennedy, and D. Reed, *J. Chem. Soc., Dalton Trans.*, 1980, 196.
3 J. E. Crook, N. N. Greenwood, J. D. Kennedy, and W. S. McDonald, *J. Chem. Soc., Chem. Commun.*, 1981, 933.
4 J. Bould, N. N. Greenwood, and J. D. Kennedy, *J. Chem. Soc., Dalton Trans.*, 1982, 481.
5 J. W. Lott and D. F. Gaines, *Inorg. Chem.*, 1974, **13**, 2261.
6 G. J. Zimmerman, L. W. Hall, and L. G. Sneddon, *Inorg. Chem.*, 1980, **19**, 3647.
7 D. F. Gaines, J. W. Lott, and J. C. Calabrese, *Inorg. Chem.*, 1974, **13**, 2419.
8 M. R. Churchill, *Perspect. Struct. Chem.*, 1971, **3**, 91.
9 W. D. Phillips, H. C. Miller, and E. L. Muetterties, *J. Am. Chem. Soc.*, 1969, **81**, 4496.
10 V. T. Aftandilian, H. C. Miller, G. W. Parshall, and E. L. Muetterties, *Inorg. Chem.*, 1962, **1**, 734.
11 J. D. Kennedy and B. Wrackmeyer, *J. Magn. Reson.*, 1980, **38**, 529.
12 S. K. Boocock, N. N. Greenwood, M. J. Hails, J. D. Kennedy, and W. S. McDonald, *J. Chem. Soc., Dalton Trans.*, 1981, 1415.
13 J. D. Kennedy and N. N. Greenwood, *Inorg. Chim. Acta*, 1980, **38**, 93.
14 S. K. Boocock, Y. M. Cheek, N. N. Greenwood, and J. D. Kennedy, *J. Chem. Soc., Dalton Trans.*, 1981, 1430.
15 L. J. Todd and A. R. Siedle, *Prog. Nucl. Magn. Reson. Spectrosc.*, 1979, **13**, 87—176.
16 S. K. Boocock, N. N. Greenwood, J. D. Kennedy, W. S. McDonald, and J. Staves, *J. Chem. Soc., Dalton Trans.*, 1980, 790.
17 S. K. Boocock, N. N. Greenwood, J. D. Kennedy, W. S. McDonald, and J. Staves, *J. Chem. Soc., Dalton Trans.*, 1981, 2573.
18 T. C. Gibb and J. D. Kennedy, *J. Chem. Soc., Faraday Trans. 2*, 1982, 525.